⌘ *Author's Choice*

THE JOURNAL OF BIOLOGICAL CHEMISTRY VOL. 286, NO. 32, pp. 28444–28455, August 12, 2011

Leucine Zipper EF Hand-containing Transmembrane Protein 1 (Letm1) and Uncoupling Proteins 2 and 3 (UCP2/3) Contribute to Two Distinct Mitochondrial Ca^{2+} Uptake Pathways*[S]

Received for publication, March 28, 2011, and in revised form, May 18, 2011 Published, JBC Papers in Press, May 25, 2011, DOI 10.1074/jbc.M111.244517

Markus Waldeck-Weiermair[‡], Claire Jean-Quartier[‡], Rene Rost[‡], Muhammad Jadoon Khan[‡], Neelanjan Vishnu[‡], Alexander I. Bondarenko[‡], Hiromi Imamura[§], Roland Malli[‡], and Wolfgang F. Graier[‡1]

From the [‡]Institute of Molecular Biology and Biochemistry, Molecular and Cellular Physiology Research Unit, Center of Molecular Medicine, Medical University Graz, Harrachgasse 21/III, 8010 Graz, Austria and the [§]Precursory Research for Embryonic Science, Japan Science and Technology Agency, 5 Sanbancho, Chiyoda-ku, Tokyo 102-0075, Japan

Cytosolic Ca^{2+} signals are transferred into mitochondria over a huge concentration range. In our recent work we described uncoupling proteins 2 and 3 (UCP2/3) to be fundamental for mitochondrial uptake of high Ca^{2+} domains in mitochondria-ER junctions. On the other hand, the leucine zipper EF hand-containing transmembrane protein 1 (Letm1) was identified as a mitochondrial Ca^{2+}/H^+ antiporter that achieved mitochondrial Ca^{2+} sequestration at small Ca^{2+} increases. Thus, the contributions of Letm1 and UCP2/3 to mitochondrial Ca^{2+} uptake were compared in endothelial cells. Knock-down of Letm1 did not affect the UCP2/3-dependent mitochondrial uptake of intracellularly released Ca^{2+} but strongly diminished the transfer of entering Ca^{2+} into mitochondria, subsequently, resulting in a reduction of store-operated Ca^{2+} entry (SOCE). Knock-down of Letm1 and UCP2/3 did neither impact on cellular ATP levels nor the membrane potential. The enhanced mitochondrial Ca^{2+} signals in cells overexpressing UCP2/3 rescued SOCE upon Letm1 knock-down. In digitonin-permeabilized cells, Letm1 exclusively contributed to mitochondrial Ca^{2+} uptake at low Ca^{2+} conditions. Neither the Letm1- nor the UCP2/3-dependent mitochondrial Ca^{2+} uptake was affected by a knock-down of mRNA levels of mitochondrial calcium uptake 1 (MICU1), a protein that triggers mitochondrial Ca^{2+} uptake in HeLa cells. Our data indicate that Letm1 and UCP2/3 independently contribute to two distinct, mitochondrial Ca^{2+} uptake pathways in intact endothelial cells.

With the introduction of sophisticated techniques that allowed direct measurements of mitochondrial Ca^{2+} signals in intact cells (1–6), the strong functional and even physical interaction of mitochondria with their cellular environment became evident (7–9). This interaction appeared to be crucial for the organelle's capability to decode and integrate cellular Ca^{2+} signals, which is an essential feature of cell signaling. Notably, convergences between mitochondria and other membrane structures allow the generation of high Ca^{2+} domains at sites of mitochondrial Ca^{2+} uptake (10, 11). It is believed that during physiological cell stimulation such high Ca^{2+} domains enable mitochondria to locally sequester Ca^{2+} via a low Ca^{2+}-sensitive mitochondrial Ca^{2+} uniporter (MCU) that was characterized as a highly selective Ca^{2+} ion channel (12). Notably, besides this low Ca^{2+}-sensitive MCU, modes of high sensitive mitochondrial Ca^{2+} uptake that operate at submicromolar Ca^{2+} ranges have been convincingly reported (13, 14). However it is not clear whether or not mitochondrial Ca^{2+} uptake is accomplished by a unique ubiquitous pathway that works at modes of different Ca^{2+} sensitivities. Alternatively, mitochondria might be equipped with different Ca^{2+} uptake machineries that achieve Ca^{2+} sequestration at different Ca^{2+} concentrations. Although the exact identity of the proteins that actually achieve Ca^{2+} transport into the mitochondrial matrix is still unclear, several recent findings confirm the latter assumption: 1) two different mitochondrial Ca^{2+} influx currents (15) and pathways (16) could be recently identified in one given cell, 2) uncoupling proteins 2 and 3 (UCP2/3)[2] were described to be involved in mitochondrial Ca^{2+} uptake in intact cells (17), 3) with the mitochondrial calcium uptake 1 (MICU1) protein a novel modulator of mitochondrial Ca^{2+} uptake was recently described in HeLa cells (18), and 4) the leucine zipper EF hand-containing transmembrane protein 1 (Letm1) was identified as a mitochondrial Ca^{2+}/H^+ exchanger that achieves a slow but highly sensitive mitochondrial Ca^{2+} loading (19). Moreover, evidence was provided that mitochondrial Ca^{2+} uptake depends on the mode and source of Ca^{2+} mobilization (14, 20, 21).

Based on recent data that indicate that UCP2/3-dependent mitochondrial Ca^{2+} uptake is involved in the rather low Ca^{2+}-

* This work was supported by the Austrian Science Funds (FWF, P20181-B05, P21857-B18, and P22553-B18). C. J.-Q. and N. V. are funded by the FWF (W 1226-B18, DKplus Metabolic and Cardiovascular Disease), and M. J. K. is funded by the FWF within the program Molecular Medicine at the Medical University of Graz.

[S] The on-line version of this article (available at http://www.jbc.org) contains supplemental Figs. S1–S3.

⌘ *Author's Choice*—Final version full access.

[1] To whom correspondence should be addressed: Institute of Molecular Biology and Biochemistry, Molecular and Cellular Physiology Research Unit, Center of Molecular Medicine, Medical University Graz, Harrachgasse 21/III, 8010 Graz, Austria. Tel.: 43-316-380-7560; Fax: 43-316-380-9615; E-mail: wolfgang.graier@medunigraz.at.

[2] The abbreviations used are: UCP2/3, uncoupling protein 2/3; ANT, adenine nucleotide translocase; $[Ca^{2+}]_{mito}$, mitochondrial Ca^{2+} concentration; Letm1, leucine zipper EF hand-containing transmembrane protein 1; MICU1, mitochondrial Ca^{2+} uptake 1; NCX_{mito}, mitochondrial Na^+/Ca^{2+} exchanger; pH_{mito}, mitochondrial pH; SOCE, store-operated Ca^{2+} entry.

sensitive mitochondrial uptake of intracellularly released Ca^{2+} but not that of entering Ca^{2+} (16, 22), and the findings that Letm1 operates as a highly sensitive Ca^{2+} uptake mechanism (19), this study was designed to investigate the particular contribution of Letm1 and UCP2/3 to mitochondrial Ca^{2+} uptake from the two major Ca^{2+} sources (*i.e.* intracellular Ca^{2+} release as well as store-operated Ca^{2+} entry, SOCE) in endothelial cells. Finally, we tested the function of MICU1 to complement an assessment of the individual role of the three most promising putative contributors to mitochondrial Ca^{2+} uptake in endothelial cells.

EXPERIMENTAL PROCEDURES

Materials—Dulbecco's modified Eagle's medium (DMEM), 2,5-di-tert-butylhydrochinone (BHQ), histamine, 2-deoxy-D-glucose, oligomycin, choline chloride, and digitonin were purchased at Sigma-Aldrich (Vienna, Austria). Fetal calf serum and media supplements were obtained from PAA Laboratories (Pasching, Austria). Fura-2/AM was ordered from Molecular Probes Europe (Leiden, Netherlands) and Transfast® reagent from Promega (Mannheim, Germany). All other chemicals were from Roth (Karlsruhe, Germany).

Cell Culture, Constructs, and Transfection—The human umbilical vein endothelial cell line, EA.hy926 passage at ≥45 stably expressing ratiometric pericam-mito (RP-mt) was used for this study. Cells were cultured in DMEM containing 10% FCS, 1% HAT (5 mM hypoxanthin, 20 μM aminopterin, 0.8 mM thymidine), 50 units/ml penicillin, 50 μg/ml streptomycin, and kept at 37 °C in 5% CO_2 atmosphere. 2–4 days before experiments cells were plated on 30 mm glass cover slips. After reaching ~80% of confluence, cells were co-transfected with different plasmids and siRNAs using Transfast® according to the protocol supplied by the manufacturer.

Buffers and Solutions—Cells were loaded with Fura-2/AM and rested prior to experiments in a Hepes-buffered solution containing (in mM): 135 NaCl, 5 KCl, 2 $CaCl_2$, 1 $MgCl_2$, 10 Hepes acid, 2.6 $NaHCO_3$, 0.44 KH_2PO_4, 0.34 Na_2HPO_4, 10 D-glucose, 0.1% vitamins, 0.2% essential amino acids, and 1% penicillin/streptomycin; pH was adjusted to 7.4 with NaOH. For experiments in intact cells the Ca^{2+}-containing experimental buffer (EB) was composed of (in mM): 138 NaCl, 5 KCl, 2 Ca_2Cl, 1 $MgCl_2$, 10 D-glucose, and 10 Hepes acid; pH was adjusted to 7.4 with NaOH. For experiments in Ca^{2+}-free solution, EB containing 1 mM EGTA instead of Ca^{2+} was used. For experiments in partially permeabilized cells, cells were perfused with 3 μM digitonin for 3 min in a high KCl buffer containing (in mM): 110 KCl, 0.5 KH_2PO_4, 1 $MgCl_2$, 20 Hepes acid, 0.03 EGTA, 5 succinate, 10 D-glucose; pH was adjusted to 7.4 with KOH. Mitochondrial Ca^{2+} uptake was triggered by the actual intracellular Ca^{2+} concentration ($[Ca^{2+}]_a$ set to 174 ± 18 nM (n = 17) (referred as "low Ca^{2+}") or to 921 ± 119 nM (n = 17) (referred as "high Ca^{2+}"): $[Ca^{2+}]_a$ was calculated from Fura-2 signals using the following equation as recently described (22): $[Ca^{2+}]_a = 350\ nM^* (F^{Ca} - F^{min})/(F^{max} - F^{Ca})$. To verify the role of the plasma membrane Ca^{2+} ATPase (PMCA), cells were stimulated with 100 μM histamine and 15 μM BHQ in a low sodium buffer (LSB) composed of (in mM): 19 NaCl, 119 choline chloride, 5 KCl, 2 $CaCl_2$ or 1 EGTA, 1 $MgCl_2$, 10 D-glucose, and 10 Hepes acid; pH was adjusted to 7.4 with KOH. For experiments using the perforated patch clamp technique the standard external solution contained (in mM): 145 NaCl, 5 KCl, 1.2 $MgCl_2$, 10 HEPES, 10 D-glucose, 2.4 $CaCl_2$. In Ca^{2+}-free solutions, $MgCl_2$ was increased to 2.2 mM and 1 mM EGTA was added. Patch pipettes were filled with a solution containing (mM): 100 KAsp, 40 KCl, 10 HEPES, 2 $MgCl_2$, 0.2 EGTA.

Isolation of Total RNA and cDNA Synthesis—Total RNA from EA.hy926 cells was isolated with the peqGold Total RNA kit (Peqlab, Erlangen). 2–3 μg of RNA were subsequently reverse transcribed to cDNA using the High Capacity cDNA Reverse Transcription kit (Applied Biosystems, Lincoln, CA).

Gene Verification—Detection of human Letm1 (Letm1, GenBank™ accession no. NM_12318.2) and human MICU1 (MICU1, GenBank™ accession no. NM_006077.2) in EA.hy926 was performed by RT-PCR. Letm1 was identified using a forward primer at position 1082 (5′-AGTTCCTCCAGGACACCATC-3′) and a reverse primer at position 1612 (5′-TCTGCAGTGTGGACTTGAGC-3′). For the verification of MICU1 (GenBank™ accession no. NM_006077.2) the forward primer at position 418 (5′-CCTGGTGAAGCAGAAGTGTT-3′) and the reverse primer at position 1151 (5′-CTCAATGCAGTGTCCACATC-3′) were used.

RNAi Design—According to already published siRNA sense sequences for Letm1 (19) and for MICU1 (18), two different siRNAs were tested in EA.hy926 cells for both genes, Letm1 and MICU1 *versus* a non-functional Control siRNA (Control): AGGUAGUGUAAUCGCCUUGtt; sense sequence for Letm1 siRNA1 (si1-Letm1): UCCACAUUUGAGACUCAGUtt and siRNA2 (si2-Letm1): AUGUUCCAUUUGGCUGCUGtt; sense sequence for MICU1 siRNA1 (si1-MICU1): GCAAUGGCGAACUGAGCAAUAtt and siRNA2 (si2-MICU1): GCAGCUCAAGAAGCACUUCAAtt. Silencing of UCP2/3 was performed using siRNAs as described and validated previously (16, 17).

Validation of siRNAs—Knock-down efficiency of functional siRNAs against human Letm1 (Ambion, Cambridgeshire, UK) or human MICU1 (Microsynth, Balgach, Switzerland) were validated individually and in combination by real-time quantitative-PCR (RTq-PCR) *versus* the Control siRNA (Microsynth, Balgach, Switzerland). 48 h after cell transfection with the respective siRNAs, mRNA was isolated and reverse transcribed. RTq-PCR was performed using specific primer pairs for human Letm1 (5′-TGTTCTTCAAGGCCATCTCC-3′, 5′-TGTTGCTGTGAAGCTCTTCC-3′), for human MICU1 (5′-CAGGTTCAGAGCATCATTCG-3′, 5′-GAACACAAGCCAGACTTGAG-3′), and QuantiTect® Primer Assays (Qiagen, Hilden, Germany), for human UCP2 (Cat. No.: QT00014140) for human UCP3 (Cat. No.: QT00017220) and for human GAPDH (Cat. No.: QT01192646) as housekeeping gene. RTq-PCR was performed with a LightCycler® 480 System (Roche, Basel, Switzerland) using the QuantiFast SYBR Green PCR kit (Qiagen).

Plasmid Constructs—Vectors for Letm1 overexpression were purchased form GeneCopoeia™ (Rockville, MD). For mitochondrial Ca^{2+} measurements the plasmid encoding the untagged Letm1 (Letm1; Cat. No.: EX-W0230-M02) was used for transfection in a ratio 3:1 with a nuclear-targeted GFP (nls-GFP). Visualization of Letm1 was done with a vector expressing

mCherry C-terminally fused to Letm1 (Letm1-mCherry; Cat. No.: EX-W0230-M56). UCP3 overexpression was achieved as previously shown (16). For ATP measurements the novel FRET-based ATP indicator AT1.03 for the cytosolic ATP and its mitochondrial-targeted version mt AT1.03 (23) for mitochondrial ATP were used.

Cytosolic Ca^{2+} and Ba^{2+} Measurements—Changes in $[Ca^{2+}]_{cyto}$ and $[Ba^{2+}]_{cyto}$ were monitored using Fura-2/AM as previously described (24, 25). Addition of Ba^{2+} to SOCE-activated cells was performed with EB using 10 mM $BaCl_2$ instead of 2 mM $CaCl_2$.

Mitochondrial Ca^{2+} and pH Measurements with Ratiometric Pericam-mito—Cells stably expressing ratiometric-pericam-mito (RP-mt) (3) were used to monitor $[Ca^{2+}]_{mito}$ and $[H^+]_{mito}$ simultaneously. RP-mt was excited at either 430 nm or 485 nm with a high-speed polychromator system VisiChrome (Visitron Systems, Puchheim, Germany). Emitted light was recorded at 535 nm using the 535AF26 emission filter from Omega Optical (Brattleboro, VT). $[Ca^{2+}]_{mito}$ was expressed as $1\text{-}F_{430}/F_0$ as previously shown (17, 26). Changes in pH were expressed as $1 - F_{485}/F_0$, where F_{485} is the fluorescence (485 nm excitation) at a given time and F_0 is the mean fluorescence of 30–60 individual measurements collected at the beginning of recordings (27). Experiments were performed at room temperature. Rates of acquisition were between 1.04 and 2.66 s and exposure times were 600–800 ms.

FRET-based Cytosolic and Mitochondrial ATP Measurements—For ATP measurements cells were transiently transfected with the FRET-based ATP indicators AT1.03 or mt AT1.03 to measure changes in cytosolic or mitochondrial ATP levels, respectively (23). The sensor was excited at 430 nm using a high-speed polychromator system VisiChrome (Vistitron Systems, Puchheim, Germany) and emission was collected at 535 and 480 nm (Versatile Filter Wheel Systems, Vistitron Systems, Puchheim, Germany).

Patch Clamp Recordings—Membrane potential was recorded using the perforated patch-clamp technique in a current clamp mode (28–32). For membrane perforation, nystatin (300 μM) was included into the pipette solution. Membrane potential was recorded using a List EPC7 amplifier (HEKA, Lambrecht/Pfalz, Germany). Borosilicate glass pipettes were pulled with a Narishige puller (Narishige Co. Ltd, Tokyo, Japan), fire-polished and had a resistance of 4–6 MΩ. The signals obtained were low pass filtered at 1 kHz, and digitized with a sample rate of 10 kHz using a Digidata 1200A A/D converter (Axon Instruments, Foster City, CA). Data collection and analysis were performed using Clampex and Clampfit software of pClamp 9 (Axon Instruments, Molecular Devices, Sunnyvale, CA).

Confocal Microscopy—High resolution imaging of cells expressing Letm1-mCherry and ratiometric pericam-mito (RP-mt) was performed using a Nipkow-disk-based array confocal laser scanning microscope (ACLSM) as described previously (17, 33). The ACLSM consisted of a Zeiss Axiovert 200 M (Zeiss 100×/1.45 oil objective, Zeiss Microsystems, Jena, Germany), equipped with VoxCell Scan® (VisiTech, Sunderland, UK), and an air-cooled argon ion laser system (series 543, CVI Melles Griot, CA). The laser line 488 nm was used to excite RP-mt, whereas alternatively wavelength 561 nm was used to excite Letm1-mCherry. Emitted light was collected at 535 nm (535AF26; Omega Optical, Brattleboro, VT) for RP-mt or 620 nm (Omega Optical) for Letm1-mCherry using a high resolution CCD camera (Photometrics CoolSNAPfx-HQ, Roper Scientific, Tucson, AZ). Acquisition and analysis were performed with Metamorph 6.2r6 (Universal Imaging, Visitron Systems, Puchheim, Germany).

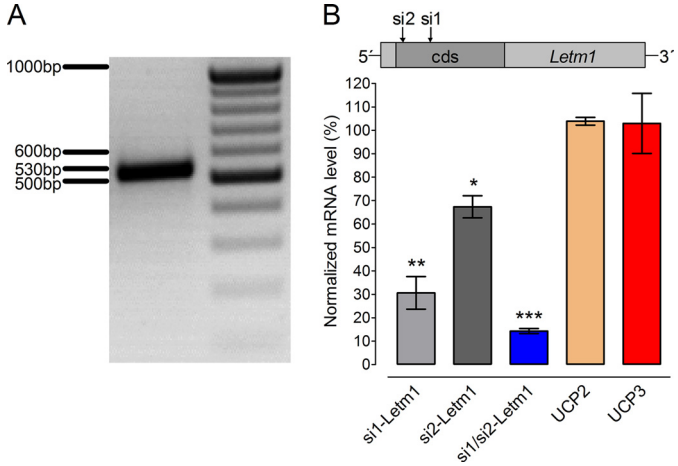

FIGURE 1. **Detection and siRNA validation of human Letm1 on the mRNA level of Ea.hy926 cells.** *Panel A*, RT-PCR using specific primers for Letm1 mRNA (see "Experimental Procedures") yielded a clear 530 bp product amplification. *Panel B*, points of applications of 2 different siRNAs (see "Experimental Procedures") against Letm1 are illustrated within the open reading frame of the mRNA of Letm1. Efficiency of siRNA-mediated Letm1 knock-down was verified by real time quantitative-PCR after transfection of siRNA1 (*si1-Letm1*, $n = 3$) or siRNA2 (*si2-Letm2*, $n = 3$) against Letm1 individually or both in combination (*si1/si2-Letm1*, $n = 3$) *versus* Control siRNA (*Control*, $n = 3$). Data are expressed in % of the maximal response in Control. *, $p = 0.013$; **, $p = 0.0019$; ***, $p < 0.0001$ *versus* Control. mRNA expression levels of either UCP2 or UCP3 were not influenced by the knock-down of Letm1 using the sample that was treated with both siRNAs against Letm1.

Statistics—Statistical data are presented as mean ± S.E. Analysis of variance (ANOVA) and Scheffe's *post hoc* F test were used for evaluation of the statistical significance. $p < 0.05$ was defined significant.

RESULTS

Letm1 Is Expressed in Endothelial Cells and mRNA Levels of Letm1 Can Be Efficiently Reduced by a Combination of Two siRNAs—Using respective primers (see "Experimental Procedures"), the expression of Letm1 was verified in the human umbilical vein endothelial cell line EA.hy926 (Fig. 1*A*). Two siRNA sequences were tested alone and in combination for the knock-down efficiency in human endothelial cells. The siRNAs reduced the mRNA level of Letm1 by 33.6 ± 4.7 ($n = 3$) and 69.4 ± 7.5 ($n = 3$) %, respectively. The combination of both siRNAs achieved the highest knock-down efficiency (85.7 ± 1.1%; $n = 3$), while they had no effect on the expression levels of UCP2 and UCP3 (Fig. 1*B*), thus, this combination was subsequently used for all experiments.

Knock-down of Letm1 and UCP2/3 Exhibit Different Inhibitory Patterns on Mitochondrial Ca^{2+} Uptake—In our previous work using the same type of cells, considerable differences in the contribution of UCP2/3 to mitochondrial Ca^{2+} sequestration were described that basically depend on the source of the Ca^{2+} supply (*i.e.* intracellular Ca^{2+} release from the ER or

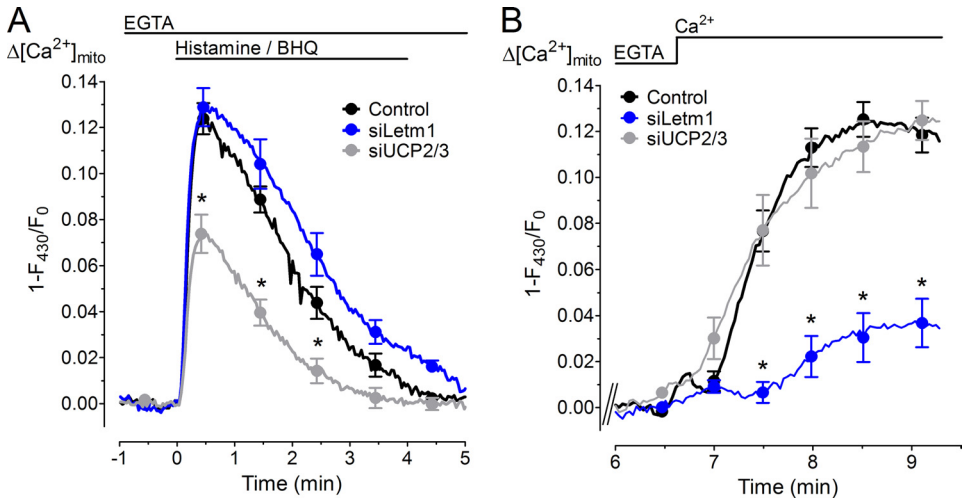

FIGURE 2. **Knock-down of UCP2/3 exclusively reduced the mitochondrial Ca^{2+} uptake from intracellularly released Ca^{2+} whereas Letm1 knock-down strongly diminished mitochondrial Ca^{2+} accumulation only upon SOCE.** Endothelial cells that stably express RP-mt cells were transiently co-transfected with nuclear GFP and either Control siRNA (*Control*: $n = 6, 14$ cells), or siRNA against Letm1 (*siLetm1*: $n = 6, 12$ cells), or siRNA against UCP2 and UCP3 (*siUCP2/3*: $n = 6, 17$ cells). Mitochondrial Ca^{2+} was measured with RP-mt. *Panel A*, knock-down of UCP2/3 but not that of Letm1 diminished mitochondrial Ca^{2+} sequestration in response to intracellular Ca^{2+} release. *, $p < 0.05$ *versus* Control. *Panel B*, knock-down of Letm1 but not that of UCP2/3 blunted mitochondrial uptake of entering Ca^{2+}. *, $p < 0.05$ *versus* Control.

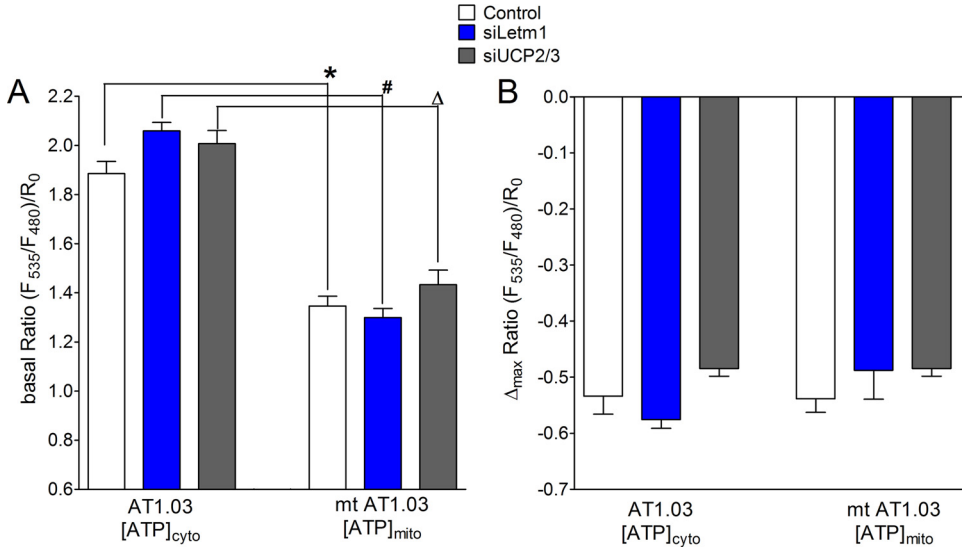

FIGURE 3. **Knock-down of Letm1 did not affect basal cytosolic and mitochondrial ATP levels or the cell's energetic activity.** Endothelial cells were transiently co-transfected with either the cytosolic ATP sensor AT1.03 or with the mitochondrial targeted mt AT1.03 together with the respective siRNAs, control siRNA (*Control*), siRNA against Letm1 (*siLetm1*) or siRNA against UCP2/3 (*siUCP2/3*). *Panel A*, basal cytosolic and mitochondrial ATP levels were neither affected by the knock-down of Letm1 nor by the knock-down of UCP2/3. *Left columns* represent the average ratio (F_{535}/F_{480}) of cytosolic ATP levels ($[ATP]_{cyto}$) at resting conditions for control cells (Control; $n = 20, 28$ cells) and cells transfected with either siRNA against Lemt1 (siLetm1; $n = 14, 15$ cells) or UCP2/3 (siUCP2/3; $n = 9, 14$ cells). *Right columns* show mitochondrial ATP levels ($[ATP]_{mito}$) for control cells ($n = 29, 32$ cells), for siLetm1 ($n = 15, 15$ cells) or siUCP2/3 ($n = 11, 17$ cells). *,#,Δ, $p < 0.05$ between respective cytosolic and mitochondrial [ATP]. *Panel B*, knock-down of Letm1 or UCP2/3 did not influence the cell's energetic activity that was initialized as shown in supplemental Fig. S1. Changes in ATP levels were calculated and expressed as Δ_{max} of Ratio (F_{535}/F_{480})/R_0 values representing $\Delta[ATP]_{cyto}$ (*left columns*) for control ($n = 13, 13$ cells), siLetm1 ($n = 6, 11$ cells) or siUCP2/3 ($n = 4, 7$ cells) and of $\Delta[ATP]_{mito}$ (*right columns*) for control ($n = 11, 11$ cells), siLetm1 ($n = 5, 6$ cells), or siUCP2/3 ($n = 5, 6$ cells) upon cell treatment with 10 mM 2-deoxy-D-glucose and 2 μM ologomycin.

entering Ca^{2+}) (16, 22). Therefore, the impact of a knock-down of Letm1 on mitochondrial uptake of intracellularly released Ca^{2+} and Ca^{2+} that is entering the cell via the store-operated Ca^{2+} entry (SOCE) was tested. For comparison, the same type of protocol was performed with cells treated with siRNAs against UCP2/3. Intriguingly, mitochondrial Ca^{2+} signals of cells reduced of either Letm1 or UCP2/3 were very different. In cells that were transiently transfected with siRNA against Letm1, no inhibitory effect on mitochondrial Ca^{2+} sequestration in response to intracellular Ca^{2+} release was found (Fig. 2*A*). The decay of the mitochondrial Ca^{2+} signal in cells treated with siRNA against Letm1 appeared to be slightly but not significantly slower, indicating that knock-down of Letm1 to some extent affects the mitochondrial Ca^{2+} extrusion process. This observation possibly points to the proposed function of mitochondrial Ca^{2+}/H^+ antiport of Letm1, which might secondly contributes to the organelle's Na^+ homeostasis. In contrast knock-down of Letm1 strongly reduced mitochondrial uptake of entering Ca^{2+} by ~80% (Fig. 2*B*). Notably, this inhibitory pattern of knock-down of Letm1 was opposite to that of

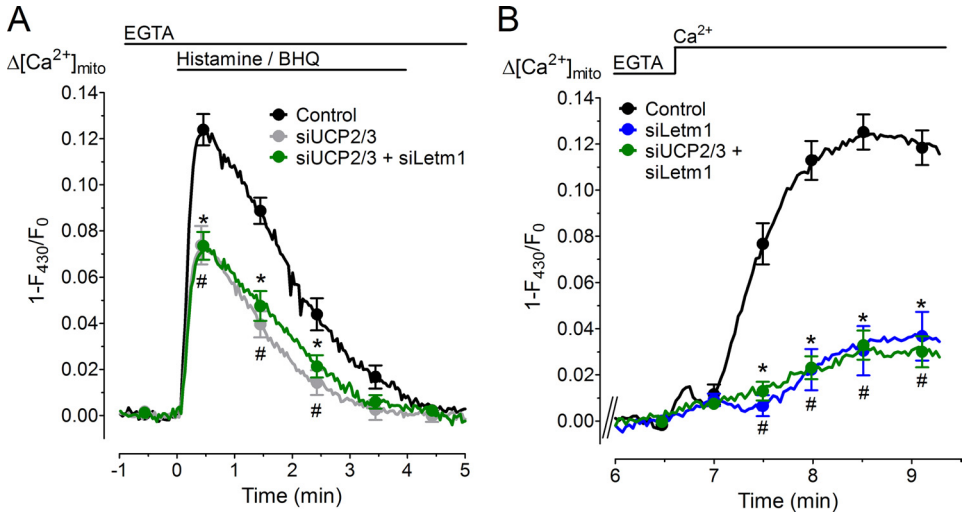

FIGURE 4. **The combined knock-down of Letm1 and UCP2/3 did not further reduce mitochondrial Ca^{2+} uptake.** Stable expressing RP-mt cells were transiently co-transfected with nuclear GFP and either Control siRNA (*Control*: $n = 6, 14$ cells) or siRNA against Letm1 (*siLetm1*: $n = 6, 12$ cells) or siRNA against UCP2 and UCP3 (siUCP2/3: $n = 6, 17$ cells) or both, siRNA against Letm1 and siRNA against UCP2 and UCP3 (siUCP2/3 siLetm1: $n = 6, 17$ cells). *Panel A*, double knock-down of Letm1 and UCP2/3 did not further reduce mitochondrial Ca^{2+} sequestration in response to intracellular Ca^{2+} release compared with that achieved by siRNA against UCP2/3 alone. *,#, $p < 0.05$ *versus* Control. *Panel B*, double knock-down of Letm1 and UCP2/3 exhibit not more inhibitory effect than the siRNA against Letm1 alone. Curves for Control and siUCP2/3 are re-plotted from Fig. 2. *,#, $p < 0.05$ *versus* Control.

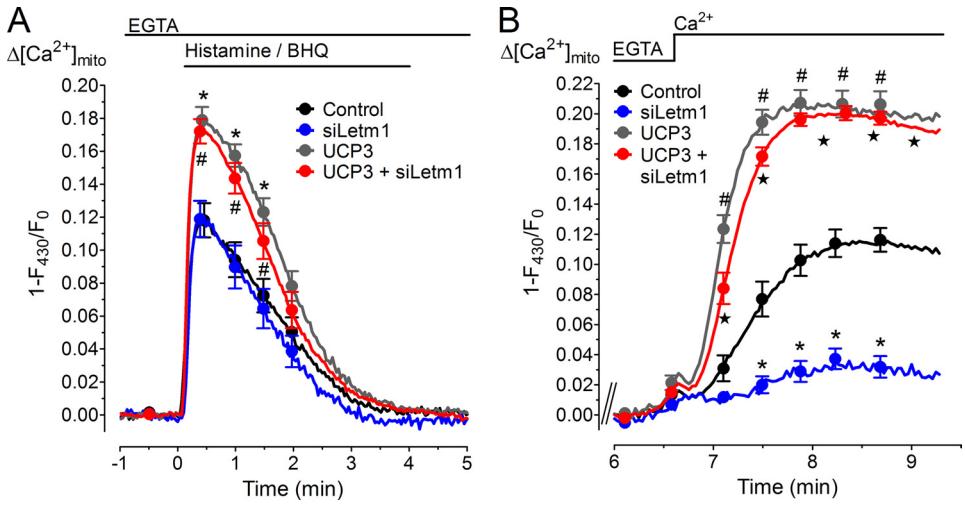

FIGURE 5. **The effect of an overexpression of UCP3 on mitochondrial Ca^{2+} sequestration was not affected by the knock-down of Letm1.** Stable expressing RP-mt cells were transiently co-transfected with nuclear GFP and either Control siRNA (*Control*: $n = 6, 16$ cells), or siRNA against Letm1 (*siLetm1*: $n = 6, 17$ cells). Overexpression of UCP3 was accomplished by co-transfecting the nuclear GFP with a plasmid coding for UCP3 in a ratio 1:3 and either Control siRNA (*UCP3*: $n = 6, 15$ cells), or siRNA against Letm1 (*UCP3 siLetm1*: $n = 6, 17$ cells). Mitochondrial Ca^{2+} was measured with RP-mt. *Panel A*, knock-down of Letm1 did not influence increased mitochondrial Ca^{2+} uptake from intracellular released Ca^{2+} upon UCP3 overexpression. *Panel B*, overexpression of UCP3 induced a strong mitochondrial Ca^{2+} entry via SOCE that was not affected by the knock-down of Letm1. Data are expressed as $1 - F_{430}/F_0$ values. *, #, ≪, $p < 0.05$ *versus* Control.

UCP2/3, which reduced mitochondrial Ca^{2+} uptake of intracellularly released but not entering Ca^{2+} (Fig. 2, *A* and *B*).

Both, Letm1 and UCP2/3-dependent Mitochondrial Ca^{2+} Signals Are Accompanied by an Acidification of the Mitochondrial Matrix—Our data so far indicate that Ca^{2+} released from the ER rapidly enters mitochondria mainly via a UCP2/3-dependent but Letm1-independent Ca^{2+} uniport. In contrast slow mitochondrial sequestration of entering Ca^{2+} appears to be primarily accomplished by Letm1, which was supposed to function as a Ca^{2+}/H^+ antiporter (19). Consequently differences of the mitochondrial proton concentration ($[H^+]_{mito}$) in response to intracellular Ca^{2+} release and Ca^{2+} entry were evaluated by using mitochondrial-targeted pericam that offers the possibility to measure changes of $[Ca^{2+}]_{mito}$ and $[H^+]_{mito}$ simultaneously (19, 26, 27). Mitochondrial Ca^{2+} elevation induced by either ER Ca^{2+} release or Ca^{2+} entry was always accompanied by increase of $[H^+]_{mito}$ (supplemental Fig. S2). These findings are in line with a recent report demonstrating decreases in mitochondrial pH that were triggered by cytosolic Ca^{2+} elevations (34). Notably, during Ca^{2+} entry mitochondrial acidification strictly correlated temporally with the raise of $[Ca^{2+}]_{mito}$, while the increase of $[H^+]_{mito}$ upon ER Ca^{2+} release occurred delayed from the mitochondrial Ca^{2+} signal (supplemental Fig. S2). Knock-down of Letm1 did not affect changes in $[Ca^{2+}]_{mito}$ and $[H^+]_{mito}$ that were induced by ER Ca^{2+} mobilization. However, in line with the data described above, cells treated with siRNA against Letm1 showed

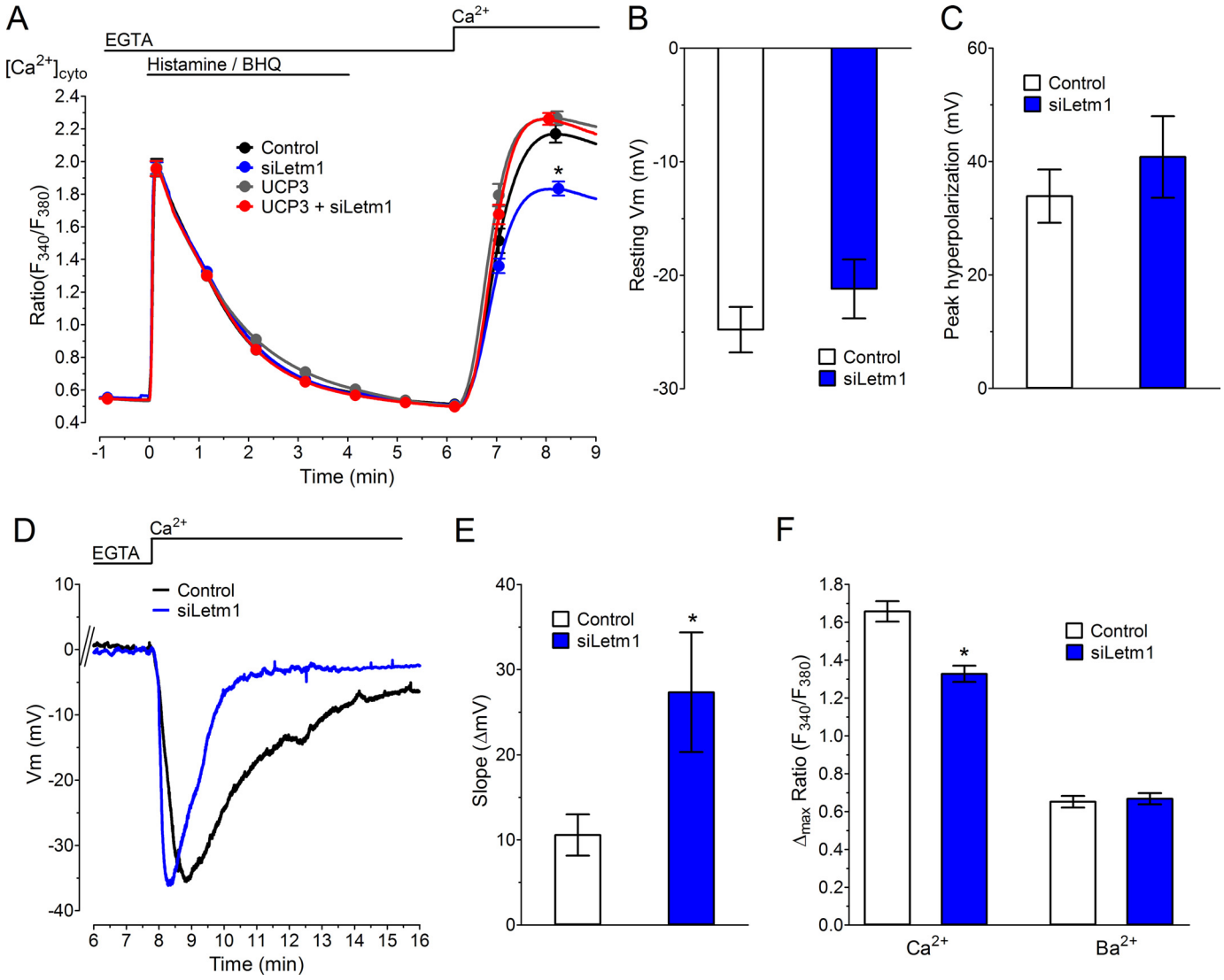

FIGURE 6. **Knock-down of Letm1 reduced the SOCE-induced cytosolic Ca^{2+} elevation that was rescued by the overexpression of UCP3, while Letm1 knock-down did not affect basal membrane potential.** *Panel A*, cells were transiently co-transfected with nuclear GFP and either Control siRNA (*Control*: n = 14, 64 cells) or siRNA against Letm1 (*siLetm1*: n = 14, 66 cells), or together with a plasmid coding for UCP3 in a ratio 1:3 and either Control siRNA (*UCP3*: n = 14, 66 cells) or siRNA against Letm1 (*UCP3 siLetm1*: n = 6, 17 cells). Cytosolic Ca^{2+} was subsequently measured after loading cells with Fura-2/AM. *, $p < 0.05$ *versus* Control. *Panels B–E*, columns and curves representing the average V_m of perforated patch-clamp recordings. *Panel B*, membrane potential at rest was recorded in controls (n = 22) and siLetm1 (n = 16). *Panel C*, peak hyperpolarization was measured after stimulation with 100 μM histamine and 15 μM BHQ in controls (n = 6) or siLetm1 (n = 7). *Panel D*, membrane potential was monitored after readdition of Ca^{2+} in controls (n = 6) or siLetm1 (n = 6). *Panel E*, slope was calculated from Ca^{2+}-induced peak hyperpolarization to 1 min thereafter in controls (n = 6) or siLetm1 (n = 6). *, $p < 0.05$ *versus* control. *Panel F*, cytosolic Ba^{2+} entry was measured in Fura-2/AM-loaded cells after the induction of maximal intracellular Ca^{2+} mobilization with 100 μM histamine and 15 μM BHQ in nominal Ca^{2+}-free solution. Columns represent the average Δ_{max} ratio (F_{340}/F_{380}) in controls (n = 14) or siLetm1 (n = 14) that was induced by addition of 2 mM Ca^{2+} to histamine/BHQ prestimulated cells. Data were analyzed from curves presented in *panel A*, *right columns* represent Δ_{max} ratio (F_{340}/F_{380}) induced by the addition of 10 mM Ba^{2+} to ER Ca^{2+}-depleted cells under control conditions (*Control*; n = 11) or in cells ablated from Letm1 (*siLetm1*; n = 11).

reduced changes in $[Ca^{2+}]_{mito}$ and $[H^+]_{mito}$ during SOCE (supplemental Fig. S2).

The Knock-down of the Mitochondrial Ca^{2+} Transporter Does Not Affect Cytosolic and Mitochondrial Basal ATP Levels—To asses cellular ATP levels, cytosolic, and mitochondrial ATP levels were recorded using FRET-based ATP sensors that are referred to as AT1.03 and mtAT1.03, respectively (23) (supplemental Fig. S1). Basal mitochondrial ATP levels were found to be significantly lower than the cytosolic ATP content in EA.hy926 cells (Fig. 3*A*), which is in line with a recent report introducing AT1.03 and mtAt1.03 investigating ATP levels of HeLa cells (23). Neither the knock-down of Letm1 nor that of UCP2/3 affected basal cytosolic or mitochondrial ATP levels (Fig. 3*A*). Similarly, the energetic activity of the cells that was indicated by the drop of cytosolic and mitochondrial ATP levels in response to 2-deoxy-D-glucose and oligomycin was not affected by knock-down of Letm1 or UCP2/3 (Fig. 3*B*).

Letm1 and UCP2/3 Independently Contribute to Different Mitochondrial Ca^{2+} Uptake Pathways in Endothelial—To test whether or not Letm1 contributes to the same mitochondrial Ca^{2+} uptake machinery than UCP2/3, the expression of these proteins was simultaneously reduced by transient transfection of a mixture of all respective siRNAs. The knock-down of Letm1 did not further reduce mitochondrial Ca^{2+} sequestration of intracellularly released Ca^{2+} in cells with a knock-down of UCP2/3 (Fig. 4*A*). In line with these findings, knock-down of

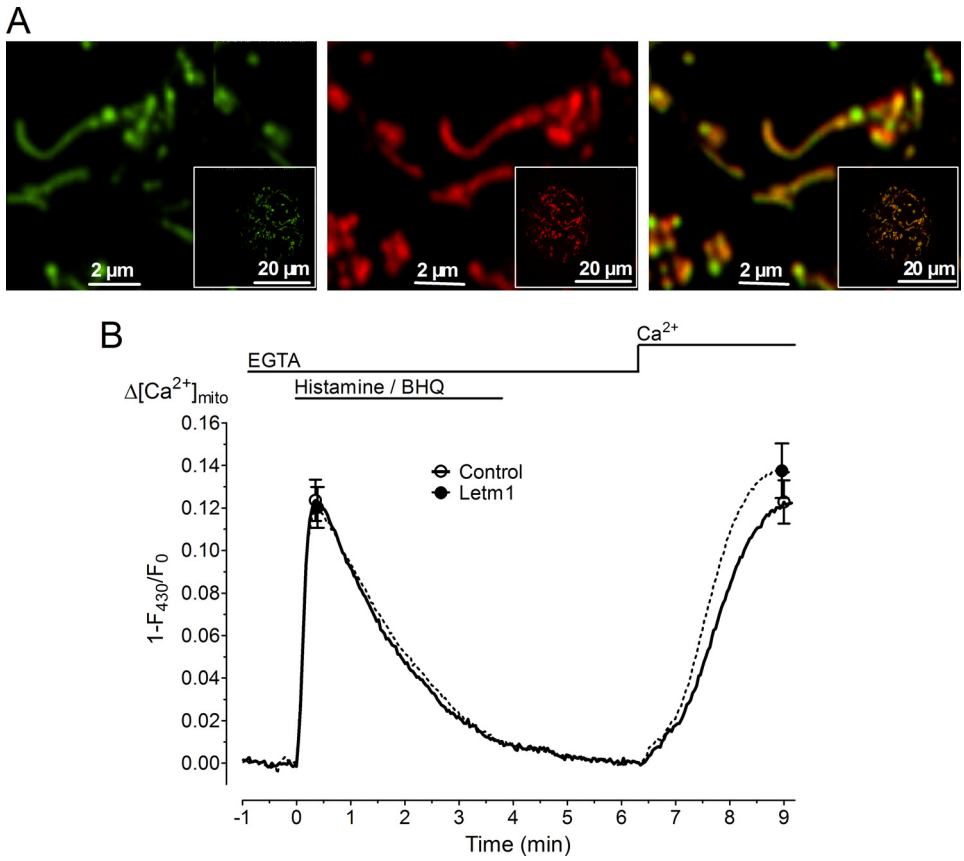

FIGURE 7. **Overexpression of Letm1 co-localized with mitochondria but did not affect mitochondrial Ca^{2+} uptake from any resources.** Plasmids encoding for Letm1-mCherry or Letm1 were transiently transfected in endothelial cells that stably express RP-mt. *Panel A*, mitochondria were visualized using RP-mt (*left panel*), Letm1 that was N-terminally tagged to mCherry was imaged to test protein targeting (*middle panel*). The overlay shows Letm1-mCherry exclusively targeted to the mitochondria (*right panel*). *Panel B*, overexpression of Letm1 did not affect mitochondrial sequestration of either intracellularly released or entering Ca^{2+}. Cells were co-transfected with Letm1 together with a nuclear-targeted GFP in a ratio 3:1 (*Letm1*: $n = 9$, 26 cells) or nuclear-targeted GFP alone (*Control*: $n = 9$, 25 cells).

UCP2/3 failed to further attenuate mitochondrial Ca^{2+} uptake of entering Ca^{2+} in cells lacking Letm1 (Fig. 4*B*).

To test whether or not UCP3 is able to compensate the diminution of Letm1, UCP3 was overexpressed in cells treated with siRNAs against Letm1. Notably, the expected augmentation of mitochondrial uptake of intracellularly released Ca^{2+} in UCP3 overexpressing cells was very robust and was not affected by Letm1 knock-down (Fig. 5*A*). As previously shown an overexpression of UCP3 almost doubled mitochondrial Ca^{2+} uptake of Ca^{2+} that enters the cells via SOCE (Fig. 5*B*). Notably, this increase of $[Ca^{2+}]_{mito}$ in cells overexpressing UCP3 remained unaffected by a knock-down of Letm1 (Fig. 5*B*).

UCP3 Overexpression Rescues a Diminished SOCE in Cells Treated with siRNA against Letm1—Mitochondrial Ca^{2+} uptake was shown to facilitate SOCE (35–39). Thus we examined the impact of Letm1 knock-down on SOCE-induced cytosolic Ca^{2+} signals. Indeed, diminution of Letm1 expression reduced the cytosolic Ca^{2+} elevation in response to SOCE, while the transient increase of $[Ca^{2+}]_{cyto}$ elicited by ER Ca^{2+} mobilization remained unaffected (Fig. 6*A*). Notably, knock-down of Letm1 reduced the SOCE induced cytosolic Ca^{2+} signal by ~20%, while the respective mitochondrial Ca^{2+} signal was reduced by almost 80%. This disparity is in line with a recent report showing that the impact of mitochondrial Ca^{2+} handling on SOCE fades with the strength of Ca^{2+} entry in this particular cell line (40). However, an overexpression of UCP3 in cells treated with siRNA against Letm1, in which an augmented mitochondrial Ca^{2+} load in response to SOCE was observed (Fig. 5*B*), completely restored SOCE-induced elevation of $[Ca^{2+}]_{mito}$ (Fig. 6*A*).

To test whether or not the reduction of SOCE due to Letm1 knock-down was caused by a possible effect on the plasma membrane potential and/or Ca^{2+}-triggered membrane hyperpolarization, electrophysiological recordings were performed. Letm1 knock-down had no effect on either the resting membrane potential (Fig. 6*B*) or peak hyperpolarization in response to Ca^{2+} readdition to histamine/BHQ prestimulated cells (Fig. 6, *C* and *D*). However, in Letm1 knock-down cells plasma membrane hyperpolarization upon Ca^{2+} addition to prestimulated cells was more transient (Fig. 6*D*) and repolarization occurred faster (Fig. 6*E*), thus, indicating that the knock-down of Letm1 yields attenuation of the maintenance of SOCE probably by the lack of the mitochondrial Ca^{2+} buffering capacity.

In agreement with this assumption, diminution of Letm1 had no effect on Ba^{2+}, which serves as Ca^{2+} surrogate for the SOCE but does not exhibit its inhibitory action on the SOC channels (Fig. 6*F*). These data further indicate that Letm1 knock-down had no effect on SOCE activation mechanisms but rather reduced its maintenance by the lack of mitochondrial Ca^{2+} buffering.

Letm1 Knock-down Does Not Affect Plasma Membrane Ca^{2+} ATPase (PMCA) Activity—Though knock-down of Letm1 did not affect cellular ATP levels, changes of cellular Ca^{2+} signals may also occur due to alterations in PMCA activity. Thus, PMCA activity was tested according to a protocol of R. S. Lewis' group that measures the decay of cytosolic Ca^{2+} upon removal of extracellular Ca^{2+} (41). We performed similar experiments in the presence of a the SERCA inhibitor BHQ, the IP3-stimulating agonist histamine, and in low Na^+ concentration to avoid ER Ca^{2+} refilling and Ca^{2+} extrusion via the plasma membrane Na^+/Ca^{2+} exchanger, respectively. These experiments revealed no effect of Letm1 knock-down on PMCA activity (supplemental Fig. S3).

In Contrast to UCP2/3, Letm1 Overexpression Fails to Improve Mitochondrial Ca^{2+} Uptake—As already shown in Fig. 4, overexpression of UCP3 yielded strong elevation in mitochondrial uptake of Ca^{2+} independently from the source it was delivered (*i.e.* intracellular Ca^{2+} release or entering Ca^{2+} via SOCE). In order to test whether an overexpression of Letm1 exhibits similar effects than that of UCP3, two Letm1 overexpression vectors according to that previously published by Jiang *et al.* (19) were designed. To verify targeting of Letm1, a mCherry-fusion construct was used that revealed targeting of overexpressed Letm1 to the mitochondria (Fig. 7*A*). Notably, neither the expression of mCherry fused Letm1 nor that of the wild-type protein had any obvious effect on mitochondrial Ca^{2+} accumulation in response to intracellular Ca^{2+} release and Ca^{2+} influx (Fig. 7*B*).

Letm1 and UCP3 Differ in Terms of Their Ca^{2+} Sensitivity—In view of the data described above that point to a distinct contribution of UCP2/3 and Letm1 to two separate mitochondrial Ca^{2+} uptake routes, the Ca^{2+} sensitivity of Letm1- and UCP2/3-dependent mitochondrial Ca^{2+} uptake was tested in digitonin-permeabilized cells. Under conditions of low Ca^{2+} application (*i.e.* 174 ± 18 nM cytosolic free Ca^{2+}; $n = 17$) (22) knock-down of Letm1 completely abolished mitochondrial Ca^{2+} sequestration, while the knock-down of UCP2/3 had no effect (Fig. 8*A*). In line with the experiments shown in Fig. 4*B*, overexpression of UCP3 boosted mitochondrial Ca^{2+} uptake even under conditions of Letm1 knock-down and established a large Ca^{2+} sequestration that did not differ from the signal in cells expressing Letm1 (Fig. 8*A*).

Challenging the permeabilized cells with a high Ca^{2+} concentration (*i.e.* 921 ± 119 nM cytosolic free Ca^{2+}; $n = 17$) (22) revealed mitochondrial Ca^{2+} uptake that was not affected by Letm1 knock-down but was markedly impaired in cells treated with siRNA against UCP2/3. Overexpression of UCP3 boosted mitochondrial uptake of high Ca^{2+} independently from the expression level of Letm1 (Fig. 8*B*). These data are in line with the findings in intact cells (Figs. 2&4) and confirm the idea of two separate mitochondrial Ca^{2+} uptake pathways: the Letm1-dependent pathway achieves mitochondrial Ca^{2+} sequestration of small capacity at relative low Ca^{2+} concentrations, while the UCP2/3-dependent mitochondrial Ca^{2+} uptake requires higher cytosolic Ca^{2+} concentrations to establish a high capacity Ca^{2+} uptake route into the organelle.

Despite Its Expression in Endothelial Cells, MICU1 Appears Not to Be Involved in Mitochondrial Ca^{2+} Sequestration in This

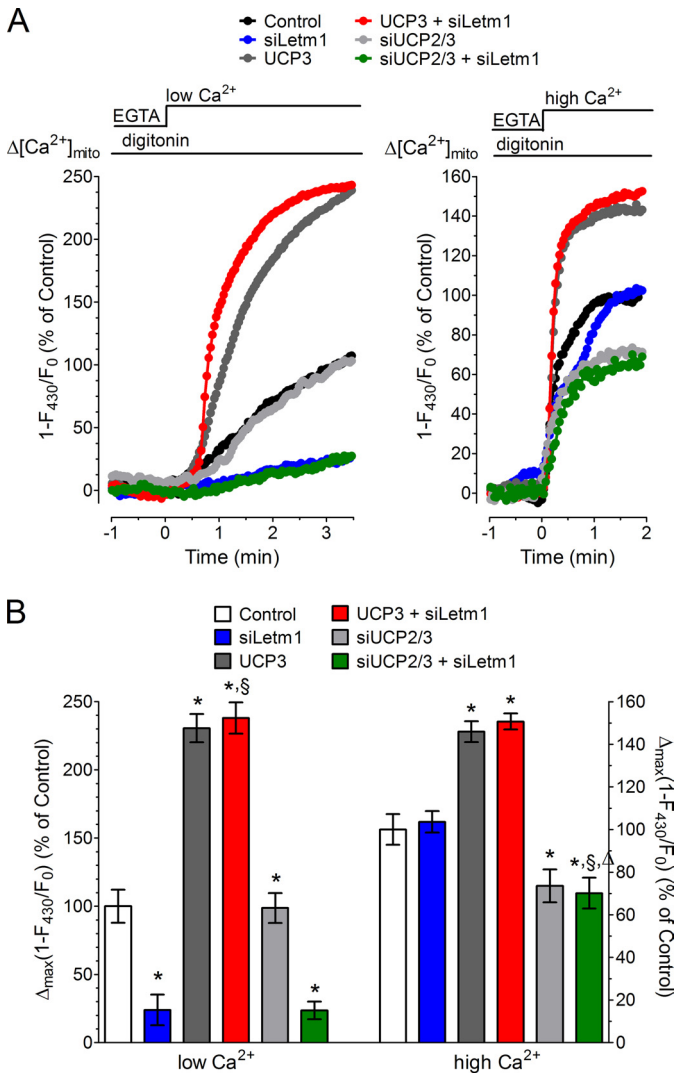

FIGURE 8. **siRNA-mediated knock-down of Letm1 and UCP2/3 had oppositional effects on mitochondrial Ca^{2+} uptake in digitonin-permeabilized cells by applying low and high Ca^{2+} concentrations, while UCP2/3 overexpression rescued mitochondrial Ca^{2+} uptake in cells with Letm1 knock-down.** Stable expressing RP-mt cells were transiently co-transfected with nuclear GFP and either Control siRNA (*Control*), siRNA against Letm1 (*siLetm1*), siRNA against UCP2/3 (*siUCP2/3*), or siRNA against UCP2/3 and Letm1 (*siUCP2/3 + Letm1*). Overexpression of UCP3 was achieved by co-transfecting the nuclear GFP with a plasmid coding for UCP3 in a ratio 1:3 and either Control siRNA (*UCP3*), or siRNA against Letm1 (*UCP3 siLetm1*). Mitochondrial Ca^{2+} was measured with RP-mt. Data are expressed as % of Control under each individual condition. *Panel A*, average curves of mitochondrial Ca^{2+} uptake upon the addition of either low Ca^{2+} concentration or high Ca^{2+} concentration in mild digitonin-permeabilized cells (Control, *black curves*; siLetm1, *blue curves*; UCP3, *light gray curves*; UCP3 + siLetm1, *red curves*; siUCP2/3 *light gray curves*; siUCP2/3 + siLetm1, *green curves*). *Panel B*, maximum mitochondrial Ca^{2+} accumulation according to the average curves of *panel A* was calculated 3.4 min after the application of low Ca^{2+} concentration and 1.8 min after applying high Ca^{2+} concentration. Columns represent the average of mitochondrial Ca^{2+} signals upon the addition of the low Ca^{2+} concentration (Control, *left white column*, $n = 4$, 12 cells; siLetm1, *left blue column*, $n = 4$, 12 cells; UCP3, *left dark gray column*, $n = 4$, 12 cells; UCP3 + siLetm1, *left red column*, $n = 4$, 12 cells; siUCP2/3, *left light gray column*, $n = 4$, 13 cells; siUCP2/3 + siLetm1, *left green column*, $n = 4$, 13 cells), and the high Ca^{2+} concentration (Control, *right white column*, $n = 4$, 10 cells; siLetm1, *right blue column*, $n = 4$, 17 cells; UCP3, *right dark gray column*, $n = 4$, 16 cells; UCP3 + siLetm1, *right red column*, $n = 4$, 13 cells; siUCP2/3, *right light gray column*, $n = 8$, 22 cells; siUCP2/3 + siLetm1, *right green column*, $n = 8$, 30 cells). *, $p < 0.05$ *versus* the respective Control; #, $p < 0.05$ between siLetm1 and UCP3 + siLetm1; §, $p < 0.05$ between siUCP2/3 and siUCP2/3 + siLetm1; and Δ, $p < 0.05$ between siLetm1 and siUCP2/3 + Letm1.

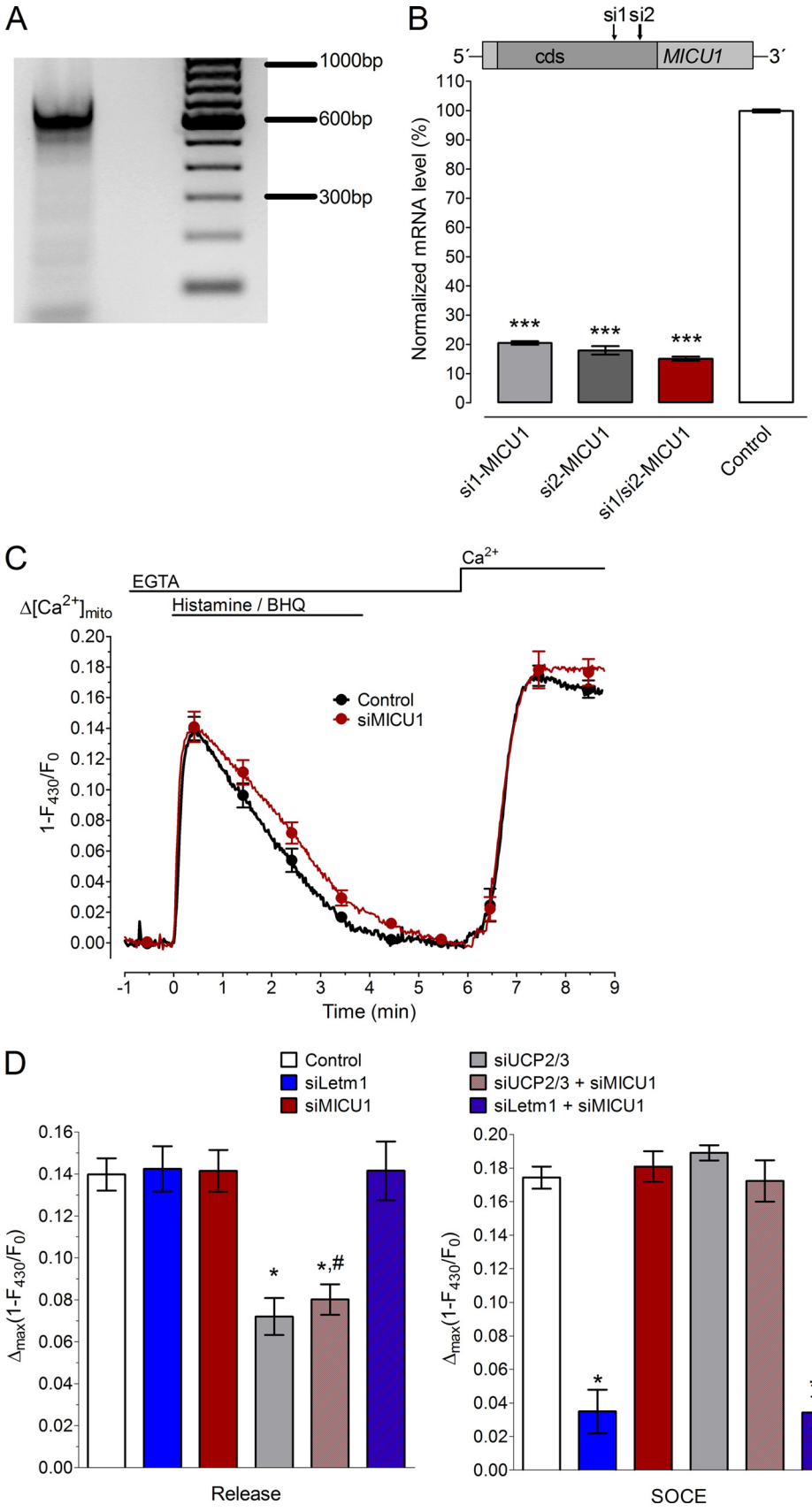
A
1000bp
600bp
300bp
B
si1 si2
5′
cds
MICU1
3′
Normalized mRNA level (%)
110
100
90
80
70
60
50
40
30
20
10
0
***
***
***
si1-MICU1
si2-MICU1
si1/si2-MICU1
Control
C
Ca2+
EGTA
Histamine / BHQ
Δ[Ca2+]mito
0.20
0.18
0.16
0.14
0.12
0.10
0.08
0.06
0.04
0.02
0.00
1-F430/F0
Control
siMICU1
-1
0
1
2
3
4
5
6
7
8
9
Time (min)
D
Control
siLetm1
siMICU1
siUCP2/3
siUCP2/3 + siMICU1
siLetm1 + siMICU1
Δmax(1-F430/F0)
0.16
0.14
0.12
0.10
0.08
0.06
0.04
0.02
0.00
*
*,#
Release
0.20
0.18
0.16
0.14
0.12
0.10
0.08
0.06
0.04
0.02
0.00
*
*,#
SOCE

Particular Cell Type—To verify the contribution of MICU1 to mitochondrial Ca^{2+} sequestration in the endothelial cell line used, the expression of MICU1 was tested using RT-PCR (Fig. 9*A*). Hence the efficiencies of the two recently published siRNAs against MICU1 (18) were measured (Fig. 9*B*). Because these experiments revealed best knock-down efficiency by a combination of both siRNAs, such approach was used in all upcoming experiments regarding MICU1 knock-down. In contrast to the knock-down of either Letm1 or UCP2/3, siRNA-mediated diminution of MICU1 mRNA levels had no effect on mitochondrial sequestration of intracellularly released as well as entering Ca^{2+} (Fig. 9*C*). Moreover, the combination of MICU1 knock-down with that of either Letm1 or UCP3 did not have any effect on mitochondrial Ca^{2+} uptake compared with that observed in MICU1-containing cells with the respective knock-down of either Letm1 or UCP2/3 (Fig. 9*D*).

DISCUSSION

Despite intensive investigations over more than a decade, the molecular identity of the mitochondrial Ca^{2+} uniporter could not be resolved entirely so far. During recent years, siRNA-based screening approaches have highlighted basically three proteins that have been found to be essential for or to contribute to mitochondrial Ca^{2+} uptake in intact cells: UCP2/3 (17), Letm1 (19), and MICU1 (18). However, in these studies mitochondrial Ca^{2+} uptake was tested under certain conditions and in distinct cell types like endothelial cells, HeLa cells (17, 18), and *Drosophila* Schneider 2 cells (19). As in other subsequent studies using different cell types and/or approaches these results were challenged, the current consensus suggests that these proteins might modulate mitochondrial Ca^{2+} uptake rather than to contribute directly to this phenomenon (42–45). Importantly, in cardiac myocytes two electrophysiological distinct Ca^{2+} uptake currents could be verified (15) that differ in terms of the Ca^{2+} range they are active, their capacity and sensitivity to ruthenium red. In agreement with this landmark publication, in our previous work, evidence was provided for the co-existence of at least two molecularly distinct mitochondrial Ca^{2+} uptake routes in the endothelial cell line EA.hy926 (16, 22, 46).

As previously published, the siRNA-mediated knock-down of UCP2/3 yielded strong reduction of mitochondrial Ca^{2+} sequestration upon intracellular Ca^{2+} release while no effect was found on mitochondrial uptake of Ca^{2+} that entered the endothelial cells via SOCE (16, 22), thus, pointing to an exclusive contribution of this particular transporter to mitochondrial Ca^{2+} sequestration at ER-mitochondria junctions in wild type endothelial cells. In this study, knock-down of Letm1, had no effect on mitochondrial Ca^{2+} uptake at ER-mitochondria junctions, but strongly diminished mitochondrial sequestration of entering Ca^{2+}, thus, indicating that the UCP2/3- and Letm1-dependent Ca^{2+} signals account for mitochondrial Ca^{2+} uptake from distinct sources (*i.e.* ER-derived intracellular Ca^{2+} release and SOCE). Our findings that the knock-down of Letm1 had no effect on Ba^{2+} entry, PMCA activity, membrane potential or basal ATP levels but diminished cytosolic Ca^{2+} elevation in response to SOCE is in line with previous reports on the considerable contribution of mitochondrial Ca^{2+} uptake/buffering for the activity/maintenance of store-operated Ca^{2+} channels (7, 26, 35–40, 47).

Because the combination of Letm1 and UCP2/3 knock-down just reflected the additive combination of the effects of the individual siRNAs, these particular mitochondrial Ca^{2+} uptake routes appear to be independent from each other. This assumption was further supported by our findings that under conditions of Letm1 knock-down, the effect of UCP3 overexpression remained unaffected. Notably, under such conditions, the overexpression of UCP3 compensated the lack of Letm1 in terms of mitochondrial sequestration of entering Ca^{2+}. These data are in agreement with our previous findings showing that overexpression of UCP2/3 establishes a respective mitochondrial Ca^{2+} uptake route also for entering Ca^{2+}, thus, pointing to the expression level of UCP3 as being the bottleneck for the establishment of a respective mitochondrial Ca^{2+} uptake.

The particular contribution of Letm1- and UCP2/3-dependent mitochondrial Ca^{2+} uptake routes to either entering Ca^{2+} or ER-released Ca^{2+} may indicate that these carriers achieve mitochondrial Ca^{2+} uptake at different Ca^{2+} concentrations. In this respect, the generation of high Ca^{2+} domains in the junction between the ER and the mitochondria to provide sufficient high Ca^{2+} levels to allow mitochondrial Ca^{2+} sequestration via the rather Ca^{2+} insensitive mitochondrial Ca^{2+} uniporter were frequently emphasized (9, 48, 49) and very recently convincingly approved (11, 50). Moreover, considerable differences in the kinetics and capacity of mitochondrial uptake of Ca^{2+} from the two major sources (*i.e.* intracellular

FIGURE 9. **siRNA-mediated knock-down of MICU1 efficiently reduced mRNA levels but had no effect on mitochondrial Ca^{2+} sequestration in endothelial cells.** *Panel A*, RT-PCR using specific primers (see "Experimental Procedures") resulted in a 733 bp product amplification, approving the expression of MICU1 in the human endothelial cell line used in this study. *Panel B*, MICU1 silencing using 2 different siRNA (single and combined). Efficiency of siRNA-mediated MICU1 knock-down was verified by real time quantitative-PCR after transfection of siRNA1 (*si1-MICU1*, $n = 3$) or siRNA2 (*si2-MICU1*, $n = 3$) against MICU1 individually or both in combination (*si1/si2-MICU1*, $n = 3$) *versus* Control siRNA (Control, $n = 3$). Data are expressed in % of Control. ***, $p < 0.0001$ *versus* Control. *Panel C*, mitochondrial Ca^{2+} uptake was not affected by MICU1 knock-down. Stably expressing RP-mt endothelial cells were transiently co-transfected with a plasmid for expression of nuclear-targeted GFP and either a Control siRNA (*Control* $n = 4$, 14 cells) or siRNA against MICU1 (*MICU1* $n = 4$, 14 cells). *Panel D*, knock-down of MICU1 did not affect mitochondrial Ca^{2+} uptake upon intracellular Ca^{2+} release or SOCE. Mitochondrial Ca^{2+} uptake was visualized by RP-mt in endothelial cells transiently expressing nuclear-targeted GFP and the respective siRNAs: Control siRNA (Control, *plain white column*, $n = 4$, 14 cells), siRNAs against Letm1 (siLetm1, *plain blue columns*, $n = 4$, 14 cells); siRNAs against MICU1 (siMICU1, *plain dark red columns*, $n = 4$, 14 cells); siRNAs against UCP2/3 (siUCP2/3, *plain light gray columns*, $n = 4$, 12 cells), siRNAs against UCP2/3 and MICU1 (siUCP2/3 + siMICU1, *dark red-striped light gray columns*, $n = 4$, 15 cells) or siRNA against Letm1 and MICU1 (siLetm1 + siMICU1, *dark red-striped blue columns*, $n = 4$, 16 cells). *Left panel*, maximal intracellular Ca^{2+} mobilization in response to 100 μM histamine and 15 μM BHQ in a nominal Ca^{2+}-free solution. Columns represent the average $\Delta_{max}\ 1-F-F_{430}/F_0$ of mitochondrial Ca^{2+} uptake upon ER Ca^{2+} release. *, $p < 0.05$ *versus* Control and #, $p < 0.05$ between siMICU1 and siUCP2/3 + siMICU1. *Right panel*, columns represent the average $\Delta_{max}\ 1-F_{430}/F_0$ of mitochondrial Ca^{2+} uptake after the addition of 2 mM Ca^{2+} to cells prestimulated with histamine and BHQ. *, $p < 0.05$ *versus* Control and #, $p < 0.05$ between siMICU1 and siLetm1 + siMICU1.

Ca^{2+} release and Ca^{2+} entry via SOCE) in endothelial cells further confirmed these data and emphasized lower Ca^{2+} concentrations at the mitochondria surface under conditions of entering Ca^{2+} than within the ER-mitochondria junction (22). The present experiments using digitonin-permeabilized cells are in agreement with these previous assumptions and indicate that in endothelial mitochondria two Ca^{2+} uptake routes exist that work either at low or high Ca^{2+} concentrations. Our findings that the siRNA-mediated knock-down of Letm1 abolished mitochondrial Ca^{2+} uptake at low but not high Ca^{2+} exposure indicates the Letm1-dependent Ca^{2+} carrier to exclusively account for mitochondrial Ca^{2+} uptake under low Ca^{2+} conditions. Considering the previous reports that entering Ca^{2+} does not generate high Ca^{2+} domains at the mitochondria surface (11, 22) these findings suggest Letm1-dependent mitochondrial Ca^{2+} uptake to account for the organelle's sequestration of Ca^{2+} that enters the cell via the SOCE. In contrast to Letm1, UCP2/3 obviously accounts for mitochondrial Ca^{2+} uptake at high Ca^{2+} concentrations. However, upon overexpression UCP3 is able to compensate the lack of Letm1 even in regard of low Ca^{2+} exposure. It seems likely that even a low active UCP2/3-dependent carrier under low Ca^{2+} load achieves mitochondrial Ca^{2+} load simply because of the largely increased amount of Ca^{2+}-carrying proteins. Notably, while the overexpression of UCP3 (and UCP2) established an increased mitochondrial Ca^{2+} uptake, an overexpression of Letm1 was without effect. Though its localization into the mitochondria was clearly approved, these findings may result from a non-functional Letm1 upon overexpression. However, as both the wild type Letm1 (transfection was controlled by co-expression of nuclear targeted GFP) as well as the FP-fusion construct failed to exhibit any effect on mitochondrial Ca^{2+} signaling, this possibility appears rather unlikely. On the other hand, Letm1 might essentially depend on (a) distinct protein(s) that are the rate-limiting factors for mitochondrial Ca^{2+} uptatke. Such multi-protein complex for mitochondrial Ca^{2+} uptake was also postulated for the UCP2/3-dependent Ca^{2+} uptake route (42, 52).

Considering that both the UCP2/3- and Letm1-dependent mitochondrial Ca^{2+} carriers might be established by a multi-protein complex rather than by the individual proteins alone, a protein that was very recently described to be involved in the regulation of mitochondrial Ca^{2+} uptake in intact cells, MICU1 (18, 43, 53), attracts great attention. However, though mRNA levels from MICU1 could be found in the endothelial cells type used in this study, approved siRNA-mediated MICU1 knock-down did not affect mitochondrial Ca^{2+} sequestration by either Letm1- or UCP2/3-dependent pathways. Accordingly, these data suggest MICU1 to be not involved in Letm1- and UCP2/3-dependent mitochondrial Ca^{2+} transport in this particular cell type. Moreover, in intact and in permeabilized cells, a knock-down of UCP2/3 could not entirely prevent mitochondrial Ca^{2+} sequestration to intracellular Ca^{2+} release and high Ca^{2+} load, respectively. Notably neither knock-down of Letm1 nor that of MICU1 further reduced mitochondrial Ca^{2+} sequestration under these conditions. Though the remaining uptake might be due to an insufficient knock-down of UCP2/3 or a modulator role rather than a carrier function of UCP2/3 in this process (7, 42), the existence of a UCP2/3-, Letm1- and MICU1-independent Ca^{2+} carrier cannot be excluded. In this respect, proteins that may not serve as Ca^{2+} carrier under physiological conditions may allow/facilitate Ca^{2+} influx into the organelle under such artificial Ca^{2+} stress conditions (*e.g.* NCX_{mito} or ANT) (42, 51).

The present findings demonstrate that at least two molecularly distinct mitochondrial Ca^{2+} uptake pathways co-exist in endothelial cells. The distinct mitochondrial Ca^{2+} uptake routes appear to be independent from the recently described modulator protein MICU1 but essentially depend on either Letm1 or UCP2/3. While further studies are necessary to investigate the specific role of each individual Ca^{2+} uptake route in physiology and pathology, this work explains mitochondrial Ca^{2+} uptake to be not a unitary process but to be established by distinct molecules, thus providing the opportunity to verify the particular contribution of each individual mitochondrial Ca^{2+} transporter to distinct physiological and pathological conditions in various cell types.

Acknowledgments—We thank Anna Schreilechner and Florian Enzinger for excellent technical assistance, Dr. A. Miyawaki (Riken, Japan) for the ratiometric pericam, N. Demaurex (University of Geneva, Switzerland) for the NLS-GFP, and Dr. C.J.S. Edgell (University of North Carolina, Chapel Hill, NC) for the EA.hy926 cells.

REFERENCES

1. Rizzuto, R., Bastianutto, C., Brini, M., Murgia, M., and Pozzan, T. (1994) *J. Cell Biol.* **126,** 1183–1194
2. Rizzuto, R., Brini, M., and Pozzan, T. (1994) *Methods Cell Biol.* **40,** 339–358
3. Nagai, T., Sawano, A., Park, E. S., and Miyawaki, A. (2001) *Proc. Natl. Acad. Sci. U.S.A.* **98,** 3197–3202
4. Filippin, L., Abad, M. C., Gastaldello, S., Magalhaes, P. J., Sandona, D., and Pozzan, T. (2005) *Cell Calcium* **37,** 129–136
5. Palmer, A. E., Giacomello, M., Kortemme, T., Hires, S. A., Lev-Ram, V., Baker, D., and Tsien, R. Y. (2006) *Chem. Biol.* **13,** 521–530
6. Palmer, A. E., and Tsien, R. Y. (2006) *Nat. Protoc.* **1,** 1057–1065
7. Demaurex, N., Poburko, D., and Frieden, M. (2009) *Biochim. Biophys. Acta* **1787,** 1383–1394
8. Rizzuto, R., Duchen, M. R., and Pozzan, T. (2004) *Sci. STKE* **2004,** re1
9. Rizzuto, R., Marchi, S., Bonora, M., Aguiari, P., Bononi, A., De Stefani, D., Giorgi, C., Leo, S., Rimessi, A., Siviero, R., Zecchini, E., and Pinton, P. (2009) *Biochim. Biophys. Acta* **1787,** 1342–1351
10. Rizzuto, R., and Pozzan, T. (2006) *Physiol. Rev.* **86,** 369–408
11. Giacomello, M., Drago, I., Bortolozzi, M., Scorzeto, M., Gianelle, A., Pizzo, P., and Pozzan, T. (2010) *Mol. Cell* **38,** 280–290
12. Kirichok, Y., Krapivinsky, G., and Clapham, D. E. (2004) *Nature* **427,** 360–364
13. Pitter, J. G., Maechler, P., Wollheim, C. B., and Spät, A. (2002) *Cell Calcium* **31,** 97–104
14. Szanda, G., Koncz, P., Várnai, P., and Spät, A. (2006) *Cell Calcium* **40,** 527–537
15. Michels, G., Khan, I. F., Endres-Becker, J., Rottlaender, D., Herzig, S., Ruhparwar, A., Wahlers, T., and Hoppe, U. C. (2009) *Circulation* **119,** 2435–2443
16. Waldeck-Weiermair, M., Malli, R., Naghdi, S., Trenker, M., Kahn, M. J., and Graier, W. F. (2010) *Cell Calcium* **47,** 433–440
17. Trenker, M., Malli, R., Fertschai, I., Levak-Frank, S., and Graier, W. F. (2007) *Nat. Cell Biol.* **9,** 445–452
18. Perocchi, F., Gohil, V. M., Girgis, H. S., Bao, X. R., McCombs, J. E., Palmer, A. E., and Mootha, V. K. (2010) *Nature* **467,** 291–296
19. Jiang, D., Zhao, L., and Clapham, D. E. (2009) *Science* **326,** 144–147
20. Spät, A., Fülöp, L., Koncz, P., and Szanda, G. (2009) *Acta Physiol.* **195,**

139–147
21. Spät, A., Szanda, G., Csordás, G., and Hajnóczky, G. (2008) *Cell Calcium* **44,** 51–63
22. Waldeck-Weiermair, M., Duan, X., Naghdi, S., Khan, M. J., Trenker, M., Malli, R., and Graier, W. F. (2010) *Cell Calcium* **48,** 288–301
23. Imamura, H., Nhat, K. P., Togawa, H., Saito, K., Iino, R., Kato-Yamada, Y., Nagai, T., and Noji, H. (2009) *Proc. Natl. Acad. Sci. U.S.A.* **106,** 15651–15656
24. Graier, W. F., Groschner, K., Schmidt, K., and Kukovetz, W. R. (1992) *Biochem. Biophys. Res. Commun.* **186,** 1539–1545
25. Graier, W. F., Paltauf-Doburzynska, J., Hill, B. J., Fleischhacker, E., Hoebel, B. G., Kostner, G. M., and Sturek, M. (1998) *J. Physiol.* **506,** 109–125
26. Malli, R., Frieden, M., Trenker, M., and Graier, W. F. (2005) *J. Biol. Chem.* **280,** 12114–12122
27. Frieden, M., James, D., Castelbou, C., Danckaert, A., Martinou, J. C., and Demaurex, N. (2004) *J. Biol. Chem.* **279,** 22704–22714
28. Bondarenko, A. (2004) *Br. J. Pharmacol.* **143,** 9–18
29. Bondarenko, A. I., Malli, R., and Graier, W. F. (2011) *Pflugers Arch.* **461,** 177–189
30. Bondarenko, A., Waldeck-Weiermair, M., Naghdi, S., Poteser, M., Malli, R., and Graier, W. F. (2010) *Br. J. Pharmacol.* **161,** 308–320
31. Frieden, M., and Graier, W. F. (2000) *J. Physiol.* **524,** 715–724
32. Frieden, M., Malli, R., Samardzija, M., Demaurex, N., and Graier, W. F. (2002) *J. Physiol.* **540,** 73–84
33. Malli, R., Naghdi, S., Romanin, C., and Graier, W. F. (2008) *J. Cell Sci.* **121,** 3133–3139
34. Poburko, D., Santo-Domingo, J., and Demaurex, N. (2011) *J. Biol. Chem.* **286,** 11672–11684
35. Hoth, M., Button, D. C., and Lewis, R. S. (2000) *Proc. Natl. Acad. Sci. U.S.A.* **97,** 10607–10612
36. Hoth, M., Fanger, C. M., and Lewis, R. S. (1997) *J. Cell Biol.* **137,** 633–648
37. Parekh, A. B. (2008) *Cell Calcium* **44,** 6–13
38. Malli, R., Frieden, M., Osibow, K., and Graier, W. F. (2003) *J. Biol. Chem.* **278,** 10807–10815
39. Malli, R., Frieden, M., Osibow, K., Zoratti, C., Mayer, M., Demaurex, N., and Graier, W. F. (2003) *J. Biol. Chem.* **278,** 44769–44779
40. Naghdi, S., Waldeck-Weiermair, M., Fertschai, I., Poteser, M., Graier, W. F., and Malli, R. (2010) *J. Cell Sci.* **123,** 2553–2564
41. Bautista, D. M., and Lewis, R. S. (2004) *J. Physiol.* **556,** 805–817
42. Graier, W. F., Trenker, M., and Malli, R. (2008) *Cell Calcium* **44,** 36–50
43. Hajnóczky, G., and Csordás, G. (2010) *Curr. Biol.* **20,** R888-R891
44. Starkov, A. A. (2010) *The FEBS J.* **277,** 3652–3663
45. Santo-Domingo, J., and Demaurex, N. (2010) *Biochim. Biophys. Acta* **1797,** 907–912
46. Trenker, M., Fertschai, I., Malli, R., and Graier, W. F. (2008) *Nat. Cell Biol.* **10,** 1237–1240
47. Parekh, A. B. (2003) *News Physiol. Sci.* **18,** 252–256
48. Rizzuto, R., Pinton, P., Brini, M., Chiesa, A., Filippin, L., and Pozzan, T. (1999) *Cell Calcium* **26,** 193–199
49. Rizzuto, R., Pinton, P., Carrington, W., Fay, F. S., Fogarty, K. E., Lifshitz, L. M., Tuft, R. A., and Pozzan, T. (1998) *Science* **280,** 1763–1766
50. Csordás, G., Várnai, P., Golenár, T., Roy, S., Purkins, G., Schneider, T. G., Balla, T., and Hajnóczky, G. (2010) *Mol. Cell* **39,** 121–132
51. Graier, W. F., Frieden, M., and Malli, R. (2007) *Pflugers Arch.* **455,** 375–396
52. Malli, R., and Graier, W. F. (2010) *FEBS Lett.* **584,** 1942–1947
53. Collins, S., and Meyer, T. (2010) *Nature* **467,** 283